

# First Principles study of electronic structure, mechanical and superconducting Properties of Palladium Hydride

## ABSTRACT

The Structural, electronic and elastic properties of mono and dihydrides of Palladium are investigated by using first principles calculation based on density functional theory as implemented in Vienna ab-initio simulation package. The calculated lattice parameters are in agreement with the experimental results. A pressure-induced structural phase transition from ZB to NaCl is observed at a pressure of 11 GPa for PdH. A high superconducting transition temperature ( $T_c$ ) of 18.76K is obtained for PdH<sub>2</sub>.

Keywords: *ab-initio calculations, structural phase transition, electronic structure, elastic properties*

PACS NO.: 31.15.A- , 61.50.Ks, 31.15.aa, 62.20.D,

## 1. INTRODUCTION

Palladium has been known as an excellent metallic absorber of hydrogen for more than a century [1]. Electronic structure of PdH<sub>0.6</sub> at 100K was studied by means of photoelectron spectroscopy [2]. Behavior of d electrons and their effect on chemical bonding for diatomic transition metal hydrides of NiH and PdH were studied [3]. PdH<sub>x</sub> is a superconductor with a transition temperature  $T_c$  of about 9 K for x=1. Band structure calculations and superconducting properties of PdH<sub>x</sub> and PdD<sub>x</sub> were reported [5]. Recently, both static and dynamic calculations of various properties of PdH(D) were performed [6]. Stoichiometric PdH and PdD in a diamond anvil cell have been synthesized and pressure dependence of the superconducting transition temperature was measured [7].

In this paper, structural, mechanical and electronic properties of mono and dihydrides of Palladium metal are investigated by the first principles calculation using Vienna ab-initio simulation package (VASP).

## 2. COMPUTATIONAL DETAILS

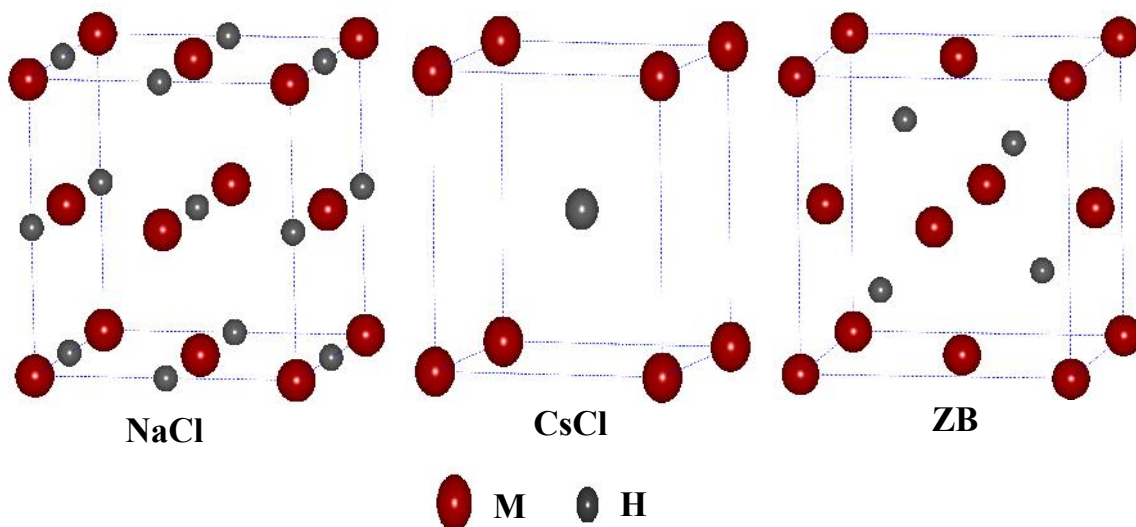
The total energy calculations are carried out using density functional theory (DFT) as implemented in the Vienna ab-initio simulation package (VASP) [8], which is based on pseudo potentials and plane wave basis functions. All electron projected augmented wave (PAW) method of Blochl [9] is applied in VASP with the frozen core approximation. The generalized gradient approximation (GGA) introduced by Perdew, Burke and Ernzerhof (PBE) [10] is employed to evaluate the electron exchange and correlation potential. The valence electron configurations are Pd 4d<sup>10</sup> and H 1s<sup>1</sup>. The cutoff energy for plane waves in our calculation is 500 eV. The integration over the Brillouin Zone (BZ) is performed with a grid of special k point-mesh determined according to the Monkhorst-Pack scheme [11] with a grid size of 8x8x8 for structural optimization and total energy calculation. Iterative relaxation of atomic positions is stopped when the change in total energy between successive steps is less than 1 meV/cell. Pressure calculations are done with second order Birch Murnaghan equation of states [12, 13]. The superconducting transition temperature is obtained using the tight binding linear muffin tin orbital method (TB-LMTO) within the framework of local density approximation (LDA) [14-17].

## 3. RESULT AND DISCUSSIONS

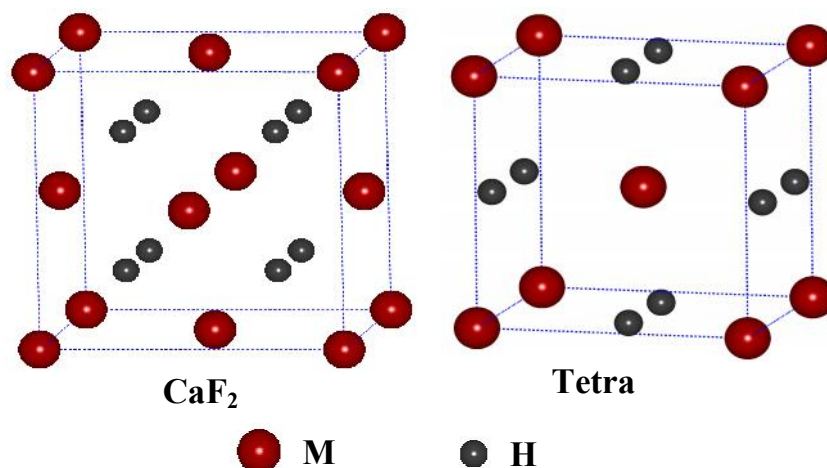
### 3.1 Geometric Properties

At ambient condition, the monohydride of palladium crystallize in ZB structure with the space group of *F-43m* (no.216). The Wyckoff positions for Pd atom is 4a:(0,0,0) and H atom is 4c:(0.25,0.25,0.25) and contains four formula units per unit cell. The dihydrides of Pd crystallize

54 in  $\text{CaF}_2$  structure with the space group of  $Fm-3m$  (no.225). The cubic unit cell is composed of  
 55 four formula units with the metal and H atoms in  $4a:(0,0,0)$  and  $8c:(0.25,0.25,0.25)$  sites  
 56 respectively. Here, each metal atom is surrounded by eight H atoms forming a cube and each  
 57 H connects with four metal atoms to build a tetrahedron. The unit cell structures of the  
 58 considered phases of mono and dihydrides of Pd atoms are given in fig. 1 (a&b).  
 59



60 Fig. 1a The unit cell structures of the considered phases of pdh  
 61  
 62  
 63



64 Fig. 1b The unit cell structures of the considered phases of PdH<sub>2</sub>  
 65  
 66

### 67 3.2 Ground State Properties

68 The stability of mono and dihydrides of Pd are analyzed by computing the formation energy using the  
 69 following relation

$$70 \Delta H_1 = E_{\text{tot}}(\text{TMH}) - E_{\text{tot}}(\text{TM}) - (1/2)E_{\text{tot}}(\text{H}_2) \quad (1)$$

$$71 \Delta H_2 = E_{\text{tot}}(\text{TMH}_2) - E_{\text{tot}}(\text{TM}) - E_{\text{tot}}(\text{H}_2) \quad (2)$$

72 where  $E_{\text{tot}}(\text{TMH}_2)$  and  $E_{\text{tot}}(\text{TMH})$  are the energies of primitive cells of  $\text{PdH}_2$  and  $\text{PdH}$   
 73 respectively.  $E_{\text{tot}}(\text{TM})$  and  $E_{\text{tot}}(\text{H}_2)$  are the energies of a transition metal atom and a hydrogen  
 74 molecule. The energy of the metal and metal hydride is calculated using VASP code, performed in  
 75 the frame work of density functional theory using the generalized gradient approximation (GGA). The  
 76 value of heat of formation  $\Delta H$  for mono and dihydrides are calculated using Equation 1 and Equation

77 2 respectively. Valence electron density (VED) is defined as the total number of valence electrons  
 78 divided by volume per unit cell. The computed lattice parameters  $a$  and  $c$  (Å), equilibrium volume  $V_0$   
 79 ( $\text{\AA}^3$ ), valence electron density  $\rho$  (electrons/  $\text{\AA}^3$ ) and cohesive energy  $E_{\text{coh}}$  (eV) for mono and dihydrides  
 80 of Pd metal for different structures are given in Table 1 along with available data [18, 19].  
 81

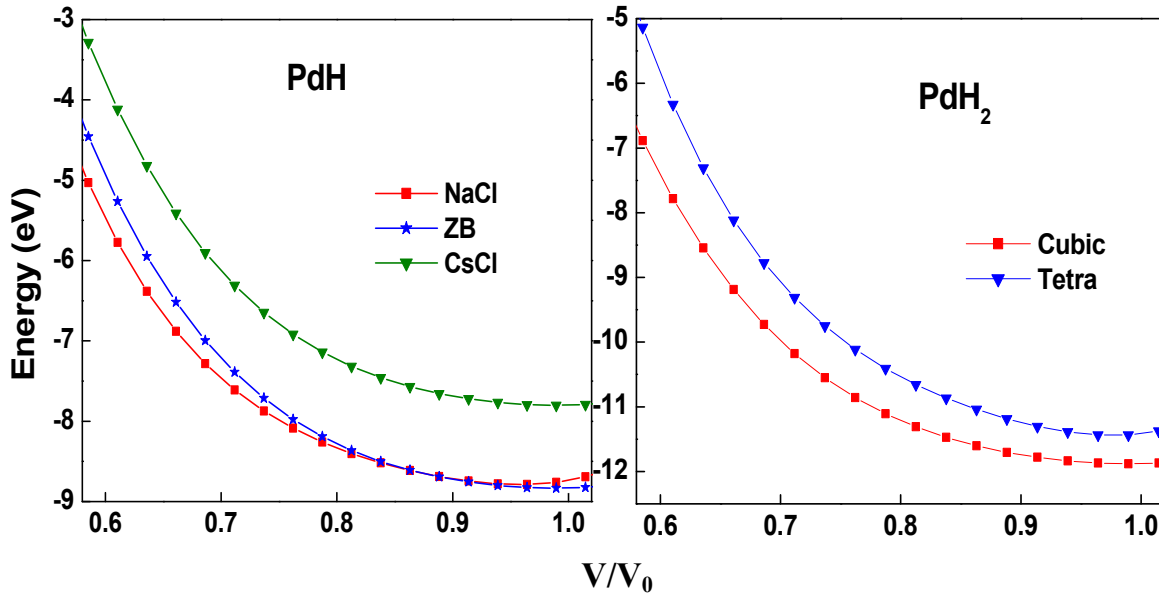
82 **Table 1 lattice parameters  $a$  and  $c$  (Å), Equilibrium  $V_0$  ( $\text{\AA}^3$ ), Valence electron density (electrons/  
 83  $\text{\AA}^3$ ) and cohesive energy  $E_c$  (eV)**  
 84

	PdH			PdH <sub>2</sub>	
	NaCl	ZB	CsCl	Cubic	Tetra
$a$	4.1440 4.07[18] 4.147[19]	4.2505	2.6746	4.475	3.7912
$c$	-	-	-	-	3.3552
$V_0$	17.820	19.240	19.130	22.40	23.46
$\rho$	0.6173	0.5717	0.5750	0.5357	0.5115
$E_c$	-4.048 -3.261[19]	-5.692	-4.02711	-4.6563	-4.0943

85  
 86  
 87  
 88  
 89  
 90  
 91

### 3.3 Structural Phase Transition

The total energy for the considered phases of mono and dihydrides of Pd is calculated as a function of reduced volume and their plots are given in Fig.2. It is noted that PdH and PdH<sub>2</sub> are stable in ZB and CaF<sub>2</sub> phases respectively. On further reducing the volume, a structural phase transition occurs from ZB to NaCl phase in PdH whereas PdH<sub>2</sub> is highly stable in the cubic (CaF<sub>2</sub>) phase at ambient and as well at high pressures.



92 **Fig.2 The total energy as a function of reduced volume for PdH and PdH<sub>2</sub>**  
 93  
 94

95 In order to determine the structural phase transition, enthalpy is calculated using the formula

$$96 H = E + PV \tag{3}$$

97 and is plotted in Fig.3. A pressure induced structural phase transition from ZB phase to NaCl phase is  
 98 predicted at a pressure of 11GPa for PdH.  
 99

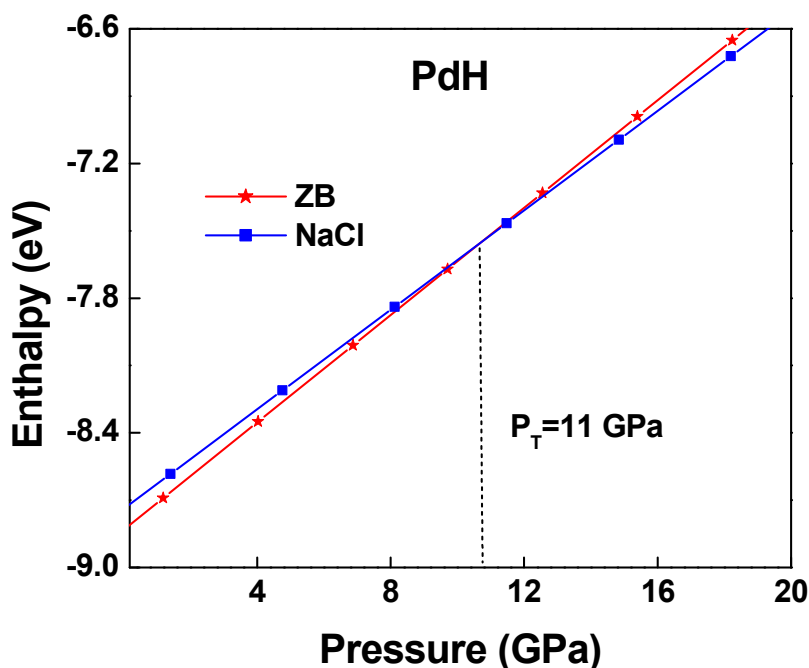


Fig.3 The enthalpy as a function of pressure of PdH

### 3.4 Elastic Properties

In order to calculate the elastic constants of a structure, a small strain is applied on to the structure and its stress is determined. The energy of a strained system [20, 21] can be expressed in terms of the elastic constants  $C_{ij}$  as:

$$\Delta E = \frac{E(\{e_i\}) - E_0}{V_0} = \left(1 - \frac{V}{V_0}\right)P(V_0) + \frac{1}{2} \left( \sum_1^6 \sum_1^6 C_{ij} e_i e_j \right) + O(\{e_i^3\}) \quad (4)$$

where  $V_0$  is the volume of the unstrained lattice,  $E_0$  is the total minimum energy at this unstrained volume of the crystal,  $P(V_0)$  is the pressure of the unstrained lattice, and  $V$  is the new volume of the lattice due to strain tensor [21]. The elasticity tensor has three independent components ( $C_{11}$ ,  $C_{12}$ ,  $C_{44}$ ) for cubic crystals. A proper choice of the set of strains  $\{e_i, i=1,2,\dots,6\}$ , in Equation (4) leads to a parabolic relationship between  $\Delta E/V_0$  ( $\Delta E \equiv E - E_0$ ) and the chosen strain. Such choices for the set  $\{e_i\}$  and the corresponding form for  $\Delta E$  are shown in Table 2 for cubic [22]. For the stable structure of mono and dihydrides of Ni and Pd at normal pressure, the lattice was strained by 0%,  $\pm 1\%$ , and  $\pm 2\%$  to obtain their total minimum energies  $E(V)$ . These energies and strains were fitted with the corresponding parabolic equations of  $\Delta E/V_0$  as given in Table 2 to yield the required second-order elastic constants.

Table 2 Strain combinations in the strain tensor for calculating the elastic constants of cubic structures

Cubic crystals		
Strain	Parameters (unlisted $e_i=0$ )	$\Delta E/V_0$
1	$e_1=e_2=\delta, e_3=(1+\delta)^{-2}-1$	$3(C_{11}-C_{12})\delta^2$
2	$e_1=e_2=e_3=\delta$	$(3/2)(C_{11}+2C_{12})\delta^2$
3	$e_6=\delta, e_3=\delta^2(4-\delta^2)^{-1}$	$(1/2)C_{44}\delta^2$

While computing these energies all atoms are allowed to relax with the cell shape and volume fixed by the choice of strains  $\{e_i\}$ . From the calculated  $C_{ij}$  values, the bulk modulus and shear modulus for the cubic crystals and hexagonal crystals are determined using the Voigt-Reuss-Hill (VRH) averaging scheme [23-25]. The strain energy  $1/2 C_{ij} e_i e_j$  of a given crystal in Equation (3) must always be positive for all possible values of the set  $\{e_i\}$ ; for the crystal to be mechanically stable. The calculated elastic

128 constants  $C_{ij}$ (GPa), Young's modulus  $E$ (GPa), shear modulus  $G$ (GPa) and Poisson's ratio ( $\nu$ ) are  
 129 listed in Table 3. From tabulated values, it is found that most of the calculated elastic constants are in  
 130 agreement with the available theoretical and experimental data [19, 26]. The small deviation in some  
 131 elastic constants may be due to the small difference in the lattice constants calculated by different  
 132 methods and also upon the various software packages used.

133 **Table 3 Elastic moduli and elastic constants in GPa**

	Pd	PdH	PdH <sub>2</sub>
$C_{11}$	358.34	184.96	197.67
$C_{12}$	206.70	241.7[19] 130.2	131.88
$C_{44}$	108.37	190.3[19] 48.53 69.05[26] 25.5[19]	31.21
$B$	257.25	148.64 183.32[26]	153.81
$G$	95.35	40.01	31.88
$E$	254.59	110.16	89.47
$\nu$	0.335	0.38	0.40

136 The Born-Huang elastic stability criteria [27] for the cubic crystals are

137 
$$C_{44} > 0, C_{11} > |C_{12}|, C_{11} + 2C_{12} > 0 \quad (5)$$

138 The computed values of the elastic constants for the rare earth metal hydrides satisfy Born-Huang  
 139 criteria suggesting that all are mechanically stable. The Young's modulus ( $E$ ) and the Poisson's ratio  
 140 ( $\nu$ ) values are two important factors necessary to find out the technological and engineering  
 141 applications of a material. The Young's modulus ( $E$ ) is given by

142 
$$E = \frac{9BG}{(3B + G)} \quad (6)$$

143 Poisson's ratio is associated with the volume change during uniaxial deformation, which is expressed  
 144 as

145 
$$\nu = \frac{C_{12}}{C_{11} + C_{12}} \quad (7)$$

146 The Debye temperature ( $\theta_D$ ) is the important parameter for determining the thermal characteristics of  
 147 materials, which correlates many physical properties of materials, such as specific heat, elastic  
 148 constants and melting temperature. The Debye temperature is defined in terms of the mean sound  
 149 velocity  $V_m$  and gives explicit information about the lattice vibrations [28] and it is calculated using  
 150 the equation [29]

151 
$$\theta_D = \frac{\hbar}{k_B} \left[ 6\pi^2 n \frac{N_A \rho}{M} \right]^{1/3} v_m \quad (8)$$

152 with  $\hbar = h/2\pi$ ,  $h$  is Planck's constant,  $k_B$  is Boltzmann's constant,  $N_A$  is the Avogadro's number,  $\rho$   
 153 is density,  $M$  is molecular weight,  $n$  is the number of atoms in the molecule and

154 
$$v_m = \left[ \frac{1}{3} \left( \frac{2}{v_t^3} + \frac{1}{v_l^3} \right) \right]^{-1/3} \quad (9)$$

155 where

156 
$$v_l = \left( \frac{B + 0.75G}{\rho} \right)^{1/2} \quad (10)$$

157 and

$$159 \quad v_t = \left( \frac{G}{\rho} \right)^{1/2} \quad (11)$$

160 are the velocities of longitudinal and transverse sound waves respectively. The calculated values are  
 161 listed in Table 4.

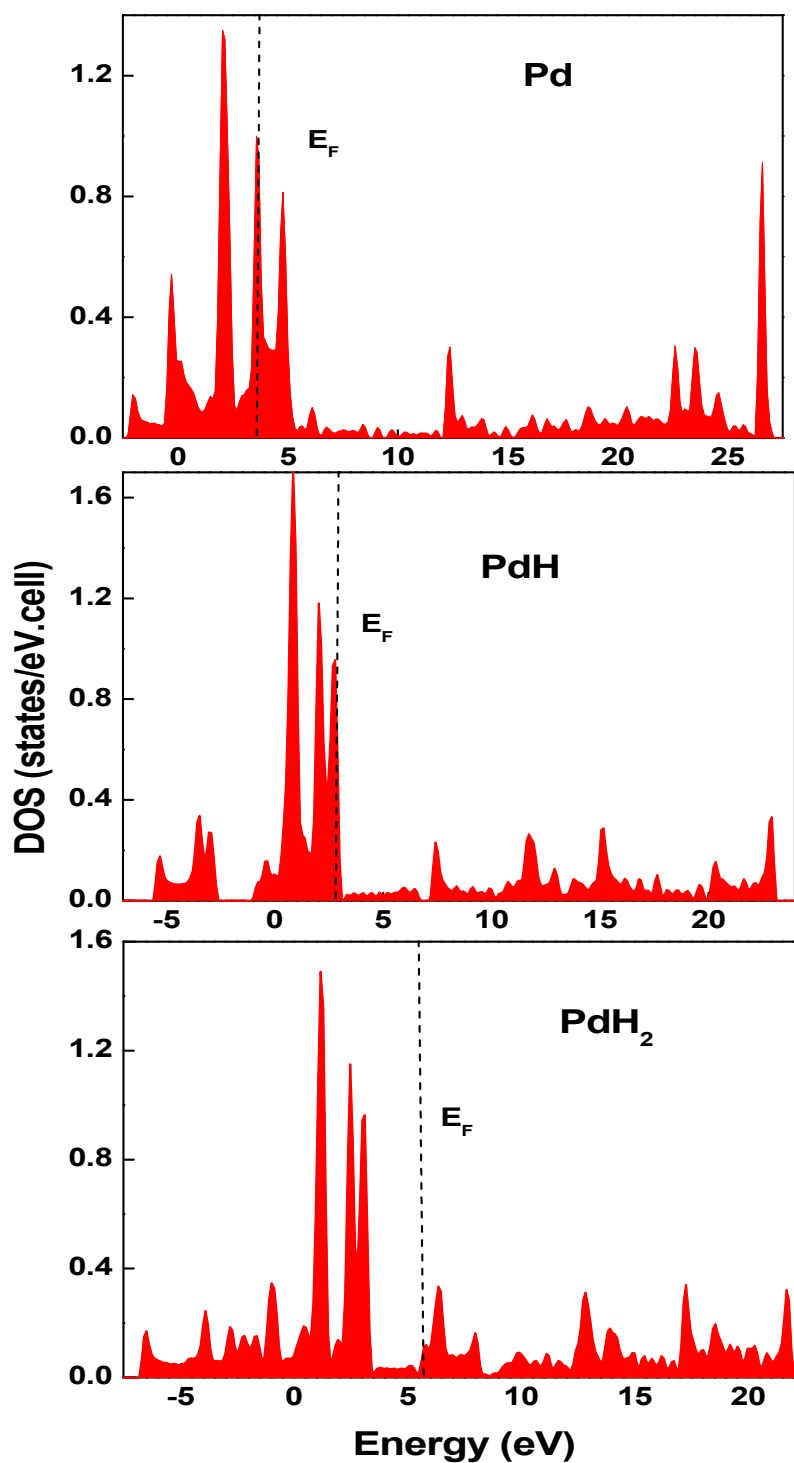
162  
 163 **Table 4 Density  $\rho$  (g/cm<sup>3</sup>), longitudinal velocity  $v_l$  (km/s), transverse velocity  $v_t$  (km/s), average**  
 164 **velocity  $v_m$  (km/s) and Debye temperature  $\theta_D$  (K) for mono and dihydrides of Pd**  
 165

	Pd	PdH	PdH <sub>2</sub>
$\rho$	12.007	9.267	8.034
$v_l$	5.644	4.645	4.943
$v_t$	2.797	2.038	1.992
$v_m$	3.139	2.301	2.256
$\theta_D$	381.59	322.25	343.74

166

### 167 3.5 Electronic Structure

168 In order to understand the electronic structure, total density of states (DOS) for the transition metal  
 169 (Pd) and for the stable structure of mono and dihydrides of Pd are given in Fig.4. The Fermi level is  
 170 indicated by a dotted vertical line. In the mono-hydrides, the hydrogen character is isolated within the  
 171 lowest peak, which is a single occupied band holding two electrons. This lowest band possesses  
 172 significant hydrogen character, in addition to a characteristic free electron tail and some metal  
 173 character. Along the series, the number of electrons in the d-state increases steadily with the increase  
 174 in the atomic number. These results indicate that a strong hybridization between the H-1s and M-d  
 175 states. The central part of the density of states (DOS) is characterized by two regions. The lower  
 176 region arises from the hybridization of p and d states of the transition metal, and the upper region is  
 177 highly dominated by 4d states. The valence states are separated by a wide gap from the occupied  
 178 states, indicating covalent behavior. Above the Fermi level the empty conduction states are present  
 179 with a mixed s, p, and d characters. Therefore at ambient pressure all these three hydrides show  
 180 metallic behavior.



181

182

Fig.4 Density of States of Pd metal, mono and dihydrides of Pd at normal pressure

183

### 184 3.6 Charge Density Analysis

185 The charge density distribution for PdH and PdH<sub>2</sub> containing M<sup>+</sup> and H<sup>-</sup> ion is shown in Fig.5. It is  
 186 observed that the voids (i.e charge depletion regions) are narrow between H ions and broad between  
 187 the metal ions. On increasing the M-ion atomic number the M-H bonding becomes stronger and these  
 188 voids change their shape. It is also found that the light colored areas indicate electron gain, whereas

189 the darker areas indicate electron loss. Because the electron gain on hydrogen is so much greater  
 190 than on the transition metal, the minimum and maximum values of electron gain and loss were  
 191 truncated, in order to keep enough resolution around the transition metals. Electron gain on the  
 192 hydrogen position is substantial, indicating that the hydrogen does not insert as a bare proton. Near  
 193 the transition metal there are both regions of positive and negative charge difference, corresponding  
 194 to the loss or gain of *d* occupation. Significant loss of *d* state electrons is observed, which is due to  
 195 the formation of a bonding-antibonding pair between the direct overlapping of hydrogen *s* with metal *d*  
 196 orbitals. A more detailed understanding of which *d* orbital's gain occupation can be obtained from the  
 197 total density of states. It is clearly seen that charge strongly accumulates between Pd and H atoms,  
 198 which means that a strong directional bonding exists between them. We can also see that the charge  
 199 around the Pd site is very much *d*-like, while that around H site is *s*-like.

200

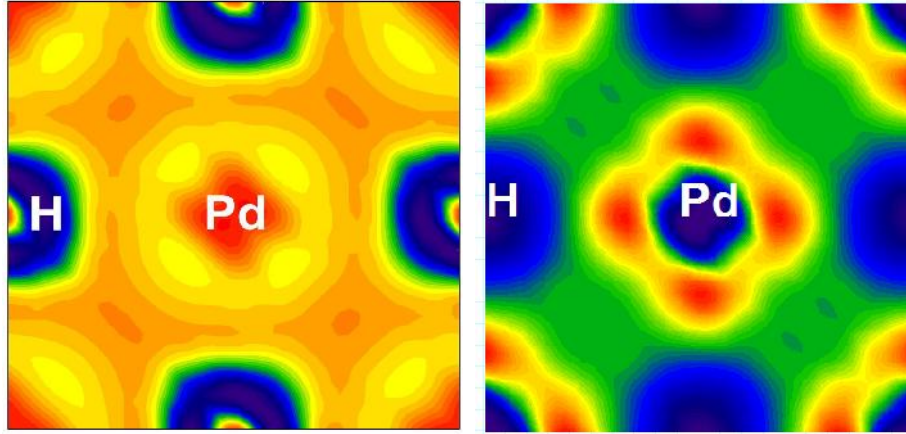


Fig.5 Charge density distribution of mono and dihydrides of Pd

201  
 202  
 203  
 204  
 205  
 206  
 207  
 208

### 3.7 Superconducting Transition Temperature ( $T_c$ K)

One of the important applications of the electronic structure calculations is the determination of the electron-phonon coupling constant, which in turn can be used to estimate the superconducting transition temperature  $T_c$ . The superconducting transition temperature is estimated by using the McMillan equation modified by Allen and Dynes [30],

$$209 \quad T_c = \frac{\omega_{\log}}{1.2} \exp \left[ \frac{-1.04(1 + \lambda)}{\lambda - \mu^* (1 + 0.62\lambda)} \right] \quad (12)$$

210 where  $\lambda$  is the electron-phonon coupling constant,  $\mu^*$  is the electron-electron interaction parameter  
 211 and  $\omega_{\log}$  is the average phonon frequency. The average of the phonon frequency square is,

$$212 \quad \langle \omega \log^2 \rangle = 0.5 \theta_D^2 \quad (13)$$

213 The variation of  $\theta_D$  with pressure in terms of ' $E_F$ ' and the lattice constant ' $a$ ' is given as,

$$214 \quad \theta_D(P) = \frac{\sqrt{E_F}}{\sqrt{E_F^0}} \frac{a_0}{a} \theta_D \quad (14)$$

215 But, in this case  $\theta_D$  is taken as constant for various pressures.  $\theta_D^0$ ,  $a^0$  and  $E_F^0$  are Debye  
 216 temperature, lattice constant and Fermi energy corresponding to normal pressure. The electron-  
 217 phonon coupling constant  $\lambda$  can be written as [31]

$$218 \quad \lambda = \frac{N(E_F) \langle I^2 \rangle}{M \langle \omega^2 \rangle} \quad (15)$$

219 where  $N(E_F)$  is the density of states at the Fermi energy.  $M$  is the atomic mass.  
 220  $\langle I^2 \rangle$  is the square of the electron-phonon matrix element averaged over the Fermi energy.  $\langle I^2 \rangle$  (in  
 221 Rydbergs) can be written as [32],



$$\langle I^2 \rangle = 2 \sum_l \left\{ \frac{(l+1)}{(2l+1)(2l+3)} \right\} M_{l,l+1}^2 \left\{ \frac{N_l(E_F)N_{l+1}(E_F)}{N(E_F)^2} \right\} \quad (16)$$

where  $M_{l,l+1}$  are the electron-phonon matrix elements which can be expressed in terms of the logarithmic derivatives.

$$D_l = \left. \frac{d \ln \phi_l}{d \ln r} \right|_{r=S} \quad (17)$$

is evaluated at the sphere boundary,

$$M_{l,l+1} = -\phi_l \phi_{l+1} \left[ (D_l(E_F) - 1)(D_{l+1}(E_F) + l + 2) + (E_F - V(S))S^2 \right] \quad (18)$$

where  $\phi_l$  is the radial wave function at the muffin-tin sphere radius corresponding to the Fermi energy. The logarithmic derivative of the radial wave function at the sphere boundary ( $D_l$ ), the muffin-tin potential at the sphere boundary ( $V(S)$ ) and the radius of the muffin-tin sphere ( $S$ ) are taken from the output of TB-LMTO program.

The electron – electron interaction parameter  $\mu^*$  is estimated using the relation [33],

$$\mu^* = \frac{0.26N(E_F)}{(1 + N(E_F))} \quad (19)$$

The calculated  $\lambda$ ,  $\mu^*$  and  $T_c$  values for PdH and PdH<sub>2</sub> at normal pressure is given in Table 5. The estimated superconducting Transition Temperature ( $T_c$ ) is 8.86 K for PdH. It is compared with the available experimental and theoretical work [34, 35, 5].

**Table 5  $\lambda$ ,  $\mu^*$  and  $T_c$  values for mono and dihydrides of Pd**

	PdH			PdH <sub>2</sub>		
	$\lambda$	$\mu^*$	$T_c(K)$	$\lambda$	$\mu^*$	$T_c(K)$
Present	0.378	0.083	8.86	1.007	0.047	18.78
Expt.			8.0[34] 9.1[35]			
Others	0.54[5]	0.085[5]	7.9[5]			

240

#### 241 4. CONCLUSION

242 The structural, electronic and elastic properties of mono and dihydrides of Pd are investigated  
 243 in detail based on first-principles calculation. Our results suggest that PdH is stable in ZB phase and  
 244 PdH<sub>2</sub> is highly stable in the CaF<sub>2</sub> phase at normal pressure. A pressure induced structural phase  
 245 transition from ZB phase to NaCl phase for PdH is predicted at a pressure of 11GPa. The calculated  
 246 superconducting Transition Temperature of PdH and PdH<sub>2</sub> is 8.86K and 18.76 at normal pressure.  
 247

#### 248 REFERENCES

- 249 1. T.Graham, Philos. Trans. R. Soc. London. 1866:156:339.
- 250 2. L.Schlapbach, J.P.Burger, J.Physique-Lettres. 1982: 43: 237.
- 251 3. Paul S.Bagus, Cecilia Bjorkman, Phys. Rev. A. 1981:23:461.
- 252 4. Tripodi, Paolo; Di Gioacchino, Daniele; Vinko, Jenny Darja. International Journal of Modern  
 253 Physics. 2007:B 21:3343–3347.
- 254 5. D.A.Papaconstantopoulos et.al, Phys. Rev. B. 1978:17:141.
- 255 6. A.Shabaev, D.A.Papaconstantopoulos et.al, Phys. Rev. B. 2010:81:184103.
- 256 7. H.Hammes et.al, Phys. Rev. B. 1989:39:4110.
- 257 8. G. Kresse, J. Furthmüller, Phys. Rev. B. 1996:54:11169.
- 258 9. P.E. Blochl, Phys. Rev. B. 1994:50:17953.
- 259 10. J.P. Perdew, K. Burke, M. Ernzerhof, Phys. Rev. Lett. 1996:77:3865.
- 260 11. H.J. Monkhorst, J.D. Pack, Phys. Rev. B. 1972:13:5188.
- 261 12. F.D. Murnaghan, The Compressibility of Media under Extreme Pressures, in Proceedings of the  
 262 National Academy of Sciences. 1944:30:244-247.
- 263 13. Francis Birch, Finite Elastic Strain of Cubic Crystals, in Physical Review. 1947:71:809-824.
- 264 14. H.L. Skriver, The LMTO method, Springer, Heidelberg. 1984.
- 265 15. O.K. Anderson, phys. Rev. B. 1975:12:3060.

- 266 16. O.K. Anderson and O. Jepsen, *phys. Rev. Lett.* 1984.53:2571.  
267 17. O.K. Anderson, O. Jepsen and M. Sob, *Electronic band structure and its applications*, Editors. M.  
268 Yussouff, Springer Verlag Lecture Notes, 1987.  
269 18. Y. Fukai, N. Okuma, *Phys.Rev.Lett.* 1994:73:1640.  
270 19. X.Zhou et.al, *J. Mat. Res.* 2008:23:704.  
271 20. J. F. Nye, *Physical Properties of Crystals*, Oxford, 1985.  
272 21. S. Q. Wu, Z. F. Hou, Z.Z. Zhu, *Solid State Commun.* 2007:143:425.  
273 22. M. Kalay, H. H. Kart, T. Çagin, *J. Alloys Compd.* 2009:484:431-438.  
274 23. W. Voigt, *Lehrbuch de Kristallphysik* (Terubner, Leipzig, 1928)  
275 24. A.Reuss, *Z.Angew, Math. Mech.* 1929:9:49.  
276 25. R.Hill, *Proc. Phys. Soc., London, Sec. A.* 1952.65:349.  
277 26. D.K.Hsu and R.G.Leisure, *Phy. Rev. B.* 1979.20:1339.  
278 27. M. Born, K. Huang, *Dynamical Theory of Crystal Lattices*, Clarendon, Oxford, 1956.  
279 28. A.M. Ibrahim, *Nucl. Instrum. Meth.B.* 1988:34:135.  
280 29. O. L. Anderson, *J. Phys. Chem. Solids.* 1963:24:909.  
281 30. P. B. Allen and R. C. Dynes. *Phys. Rev. B.* 1975:12:905.  
282 31. W. L. McMillan, *Phys. Rev. B.* 1968:167:331.  
283 32. H. L. Skriver, I. Mertig, *Phys. Rev. B.* 1985:32:4431.  
284 33. K.H. Bennemann, J.K.Garland, *Superconductivity in d and f- Band metals*, in: D.H. Douglass  
285 (Ed.), *American Institute of Physics*, Newyork, 1971.  
286 34. J.E. Schirber and C.J.M. Northrup, *Phy. Rev. B.* 1974:10:3818.  
287 35. R.J. Miller and C.B. Satterthwaite, *Phy. Rev. Lett.* 1975:34:3818.